Elastic scattering of protons from ^{15}N

R. J. deBoer,[1,*] P. J. LeBlanc,[1,†] S. Falahat,[1,2] G. Imbriani,[1,3] J. Görres,[1] S. O'Brien,[1] E. Uberseder,[1] and M. Wiescher[1]

[1]*Department of Physics, University of Notre Dame, Notre Dame, Indiana, USA*
[2]*Max Planck Institut für Chemie, Mainz, Germany*
[3]*Università degli Studi di Napoli "Federico II" and INFN, Napoli, Italy*

Background: Resonances observed through elastic scattering of protons on ^{15}N can provide information about the partial widths, spin parities, and energies of excited states in ^{16}O near the proton separation energy. This is the same energy region important for the nuclear astrophysics reactions ^{15}N$(p,\gamma)^{16}$O and ^{15}N$(p,\alpha)^{12}$C. While previous measurements have been made, they are limited in scope, especially in their angular coverage. **Purpose:** Obtain additional ^{15}N$(p,p)^{15}$N reaction data which can be used in a global multiple-channel R-matrix analysis of the ^{16}O compound nucleus in order to better constrain the level parameters of states which contribute to the reaction ^{15}N$(p,\gamma)^{16}$O. **Methods:** Measure the excitation functions of ^{15}N$(p,p)^{15}$N over an energy range from $E_p = 0.6$ to 1.8 MeV at laboratory angles of 90°, 105°, 135°, 150°, and 165°. The reaction ^{15}N$(p,\alpha_0)^{12}$C was measured concurrently. **Results:** Ratios of the excitation functions were extracted from the yield data. Resonances were identified in the yield ratio data which correspond to previously reported levels in ^{16}O. An R-matrix analysis, which fits the present data as well as previous measurements from the literature simultaneously, finds reasonable agreement between the current measurements and those in the literature. **Conclusions:** The additional data from this measurement will be combined with previous literature data in a comprehensive R-matrix analysis of reactions which populate ^{16}O over a similar energy region.

The reactions ^{15}N$(p,\gamma)^{16}$O and ^{15}N$(p,\alpha)^{12}$C form a branch point for the CNO bi-cycle [1,2]. A determination of the relative reaction rates is necessary for modeling stellar energy production and the nucleosynthesis of carbon, nitrogen, and oxygen isotopes in stellar hydrogen burning. It is presently impossible to directly measure the reaction cross sections at stellar energies because of the rapidly decreasing Coulomb penetrability. For this reason extrapolations of the cross section obtained at higher energies are typically used to estimate the rates. The level of accuracy of these extrapolations depends on an accurate description of the reaction mechanism determining the cross section. In the case of low-energy proton capture on ^{15}N, the cross section is dominated by broad interfering resonances, which must be investigated over a wide energy range so that resonance interferences can be determined and so that the tails of broad, higher-energy resonances may be accurately included.

Proton unbound states in ^{16}O, populated by resonant proton capture on ^{15}N, can deexcite through several decay channels, by proton emission to the ground state of ^{15}N, α emission to either the ground state or first excited state of ^{12}C, and γ emission(s) to lower-lying states in ^{16}O. The cross section for the different reaction channels can be formulated in terms of R-matrix theory, as a function of the resonance energies, the partial decay probabilities or widths, and the spin parity for each resonance. The analysis of the ^{15}N$(p,\gamma)^{16}$O [3] reaction requires an accurate determination of these level parameters. Since compound nucleus reactions are described by the same level parameters, we utilized the ^{15}N$(p,p)^{15}$N elastic scattering reaction to constrain the level parameters important for describing the other reaction channels.

Only two previous studies have been performed for elastic proton scattering on ^{15}N at low proton energies. Both studies mapped the excitation curve over a certain energy range: Hagedorn (1957) [4] from $E_p = 0.6$–1.8 MeV at $\theta_{\text{lab}} = 86.2°$, 122.0°, and 158.7°, and Bashkin *et al.* (1959) [5] from $E_p = 1.0$–3.7 MeV at $\theta_{\text{lab}} = 86.2°$ and 159.5°. Both measurements are in reasonable agreement but only cover a limited angular range. In addition, the data do not exist in tabulated form for either measurement and must be digitized from figures in those works. Individual data point uncertainties are also not given, making a statistically significant R-matrix fit to the data more difficult.

In order to verify and improve on the previous measurements, elastic proton-scattering excitation curves have been measured over the laboratory proton energy range $E_p = 0.6$–1.8 MeV at laboratory angles of $\theta_{\text{lab}} = 90°$, 105°, 135°, 150°, and 165°. Concurrently, ^{15}N$(p,\alpha_0)^{12}$C data were measured. The experiment and preliminary analysis are discussed in the following sections.

The ^{15}N$(p,p)^{15}$N and ^{15}N$(p,\alpha_0)^{12}$C measurements were performed at the University of Notre Dame's Nuclear Science Laboratory (NSL) using a 4-MV KN Van de Graaff accelerator which provided proton beams over the energy range $E_p = 0.6$–1.8 MeV. Beam intensities were typically $\sim$10 μA. The energy calibration of the Van de Graaff was established to better than 1 keV using the well-known ^{27}Al$(p,\gamma)^{28}$Si resonance at 0.992 MeV [6].

The windowless gas target system RHINOCEROS [7] was used as the target system for this experiment. This gas target

———
*rdeboer1@nd.edu
†Current address: Canberra Industries, Inc., 800 Research Parkway, Meriden, CT 06450, USA.
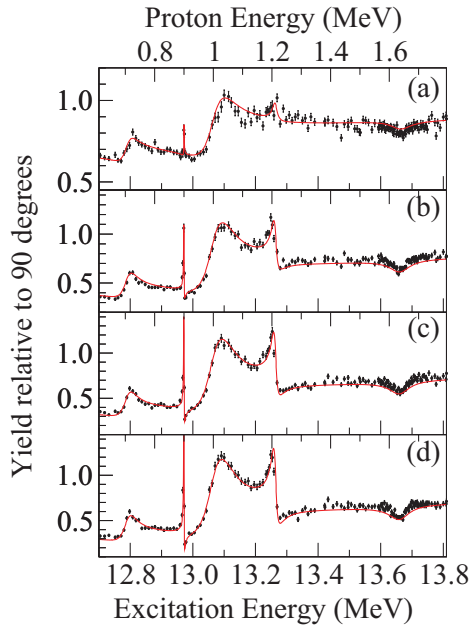
FIG. 1. (Color online) R-matrix fits to the $^{15}N(p,p)^{15}N$ yield ratio data of this work at $\theta_{lab} = 105°$, $135°$, $150°$, and $165°$ [labeled a) through d), respectively]. The data are fit simultaneously with cross-section data from the literature (see text). The yield ratios are in the center-of-mass frame.

has been used extensively in the past (see, e.g., Refs. [8,9] and references therein for further details). Nitrogen gas, enriched to 99% ^{15}N and kept at a pressure of $\sim$0.25 Torr, was used throughout the experiment. The target chamber was very similar to the one shown in Ref. [9]'s Fig. 2 a, except that additional view ports were available at $\theta_{lab} = 135°$, $150°$, and $165°$. Silicon surface barrier detectors were mounted at $\theta_{lab} = 90°$, $105°$, $135°$, $150°$, and $165°$ approximately 6 cm from the center of the gas target. Collimators of varying diameter and slits of various separations were placed in front of each detector to define the solid angle $d\Omega$ and the effective path length l. The general layout of the gas target setup was the same as that described in Ref. [10]. Values of the geometric quantity $ld\Omega$ were made similar for each detector in order to achieve the same product of detector efficiency times target density.

Because of the kinematic resolution of the setup, α particles from the reaction $^{15}N(p,\alpha_1)^{12}C$ could not be easily separated from scattered protons. In order to prevent these low-energy α particles from reaching the detector, nickel foils with a thickness of 0.75 μm were placed in front of each detector.

For each detector, yields were extracted for both the reactions $^{15}N(p,p)^{15}N$ and $^{15}N(p,\alpha_0)^{12}C$. Because gas target systems effect the charge of the initial particle beam, Faraday cup charge collection was not a reliable method for determining the integrated number of incident beam particles. For this reason only the ratios of the yields were determined and analyzed to extract the resonance structure of ^{16}O. Because the measurements for each detector were done simultaneously, taking the ratio of the yields eliminates the need for absolute measurement of the number of incident beam particles or the number of gas target nuclei. The $^{15}N(p,p)^{15}N$ cross section has been well measured at angles close to $90°$ [4,5]; therefore this angle was chosen as the angle of reference. The relative geometric factors ($ld\Omega$) were determined from the yields at the peak of the 1^- resonance at $E_p = 1.034$ MeV, which has been shown to be isotropic, at $90°$ and more backward angles, to an accuracy of $\sim$10% [4,11]. Therefore, a systematic uncertainty of 10% is recommended for the $^{15}N(p,p)^{15}N$ and $^{15}N(p,\alpha_0)^{12}C$ yield ratio data of this work.

The yields for the $105°$, $135°$, $150°$, and $165°$ detectors, each divided by the yield from the $90°$ detector, are shown in Fig. 1 for the reaction $^{15}N(p,p)^{15}N$ and Fig. 2 for the reaction $^{15}N(p,\alpha_0)^{12}C$. Because the cross section for $^{15}N(p,\alpha_0)^{12}C$ decreases substantially between $E_p = 1.4$ and 1.8 MeV, statistics limited the measurement of the $^{15}N(p,\alpha_0)^{12}C$ yields to below $E_p = 1.4$ MeV.

The present yield ratios were analyzed with the R-matrix code AZURE [12,13]. $^{15}N(p,p)^{15}N$ cross-section data from Refs. [4,5], $^{15}N(p,\alpha_0)^{12}C$ cross-section data from Refs. [5,14–18], and $^{12}C(\alpha,\alpha_0)^{12}C$ cross-section data from Ref. [19] were fit simultaneously with the yield ratio data of this work. The thin target approximation is well satisfied over most of the experimental energy region. The exception to this is over the region of the narrow, $\Gamma_{total} \approx 1$ keV, 2^- resonance at $E_x = 12.97$ MeV. For this reason, the level parameters for this resonance were fixed to previous reported values [20]. Excluding this narrow resonance, good agreement

TABLE I. Level parameters for the R-matrix analysis describing the resonances observed in this work compared to those in the literature [20]. Uncertainties of the parameters will be evaluated in a forthcoming publication [21]. The 2^- resonance was included but was not fit. Its parameters were fixed to those from the literature.

| J^π	This work					Compilation [20]			
	E_p (MeV)	E_x (MeV)	Γ_{α_0} (keV)	Γ_{α_1} (keV)	Γ_p (keV)	E_x (MeV)	Γ_{α_0} (keV)	Γ_{α_1} (keV)	Γ_p (keV)
0^-	0.713	12.796			56	12.796(4)			40
2^+	0.895	12.966	350	1.2	1.6	13.020(10)	150(10)		3
2^{-a}						12.9686(4)		0.30(6)	1.04(7)
1^-	1.034	13.097	28.8	0.6	121.4	13.090(8)	40(18)	1	100
3^-	1.082	13.142	72.8	21.3	1.2	13.129(10)	90(14)	20	1
3^-	1.218	13.269	14.0	10.7	3.2	13.259(2)	9(4)	8.2(11)	4.1
1^+	1.640	13.665		60.3	9.2	13.664(3)		59(6)	10

[a]Resonance parameters fixed at values from the literature [20].
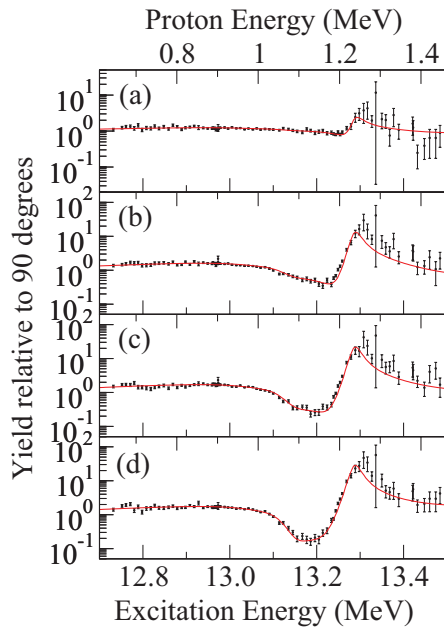
FIG. 2. (Color online) R-matrix fits to the $^{15}N(p,\alpha_0)^{12}C$ yield ratio data of this work at $\theta_{lab} = 105°, 135°, 150°$, and $165°$ [labeled a) through d), respectively]. The data are fit simultaneously with cross-section data from the literature (see text). The yield ratios are in the center-of-mass frame.

FIG. 3. (Color online) R-matrix fits to the $^{15}N(p,p)^{15}N$ cross-section data from Ref. [4] (circles) at $\theta_{lab} = 86°, 122°$, and $159°$ [labeled a) through c), respectively] and from Ref. [5] (pluses) at $\theta_{lab} = 86°$ and $159°$ [labeled a) and c), respectively]. The data are fit simultaneously with the yield ratios of this work and other cross-section data from the literature (see text). Since individual uncertainties are not provided in Refs. [4,5], an uncertainty of 3% has been assumed for each data point. Cross sections are in the center-of-mass frame.

between the current and literature data was obtained using previously determined spin-party assignments. There seems to be some difference in the energy dependence of the literature data at higher energy, but the extent of the disagreement is difficult to quantify since uncertainties are not given. The $^{15}N(p,p)^{15}N$ yield ratios clearly resolve five resonances at E_x $(J^\pi) = 12.796(0^-), 12.966(2^-), 13.097(1^-), 13.269(3^-)$, and $13.665(1^+)$ MeV. In addition to the two natural parity resonances observed in the $^{15}N(p,p)^{15}N$ data, two additional broad natural parity states, at E_x $(J^\pi) = 13.142$ (3^-) and $12.966(2^+)$ MeV, are necessary in order to reproduce the $^{15}N(p,\alpha_0)^{12}C$ data.

The level parameters extracted from the R-matrix fit are given in Table I. Most were found to be in reasonable agreement with those given in the literature [20]. The one significant exception to this is the α_0 width of the broad 2^+ resonance, which is found to be nearly 200 keV larger than the value listed in the compilation. This larger value of the width is the result of a complete R-matrix treatment of the $^{12}C(\alpha,\alpha_0)^{12}C$ data. The value from the literature is an average of past Breit-Wigner analyses which do not include interference effects and would have trouble isolating this level from the other nearby broad resonances.

The R-matrix fits are shown by the solid red lines in Figs. 1, 2, and 3, illustrating the level of consistency of the
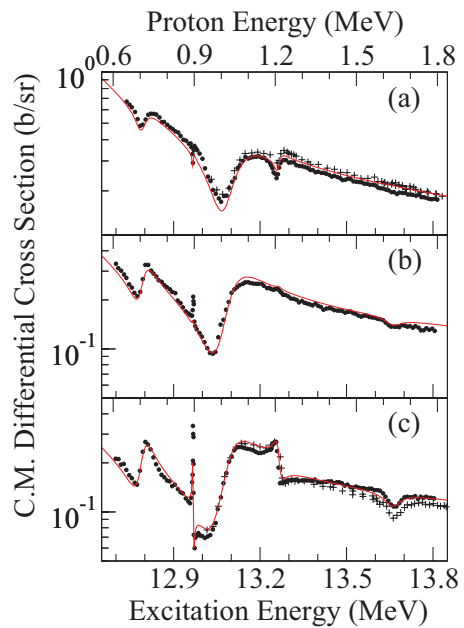
simultaneous fit of the present data together with the literature data. Calculation of the level parameter uncertainties will be presented in a forthcoming publication [21] where the current data are combined with additional literature data in a global R-matrix analysis.

In conclusion, measurements for the reactions $^{15}N(p,p)^{15}N$ and $^{15}N(p,\alpha_0)^{12}C$ at the University of Notre Dame's NSL were performed using the gas target system RHINOCEROS. Yield ratios were extracted from the measurements, and a preliminary R-matrix analysis was performed demonstrating the level of consistency with previous absolute measurements. These measurements substantially increase the amount of data available for the reaction $^{15}N(p,p)^{15}N$ in this low-energy region. In a future publication [21], the data will be combined in a global R-matrix analysis of the compound nucleus ^{16}O, which will be used to more accurately extrapolate the cross section of the reaction $^{15}N(p,\gamma_0)^{16}O$ to stellar energies.

[1] G. R. Caughlan and W. A. Fowler, Astrophys. J. **136**, 453 (1962).

[2] M. Wiescher, J. Görres, E. Uberseder, G. Imbriani, and M. Pignatari, Annu. Rev. Nucl. Part. Sci. **60**, 381 (2010).

[3] P. J. LeBlanc, G. Imbriani, J. Görres, M. Junker, R. Azuma, M. Beard, D. Bemmerer, A. Best, C. Broggini, A. Caciolli *et al.*, Phys. Rev. C **82**, 055804 (2010).

[4] F. B. Hagedorn, Phys. Rev. **108**, 735 (1957).

[5] S. Bashkin, R. R. Carlson, and R. A. Douglas, Phys. Rev. **114**, 1543 (1959).

[6] J. Keinonen and A. Anttila, Comment. Physico-Math. **46**, 61 (1976).

[7] J. Hammer, W. Biermayer, T. Griegel, H. Knee, and K. Petkau, *RHINOCEROS, The Versatile Stuttgart Gas Target Facility (Part I)* (unpublished).

[8] M. Jaeger, R. Kunz, A. Mayer, J. W. Hammer, G. Staudt, K. L. Kratz, and B. Pfeiffer, Phys. Rev. Lett. **87**, 202501 (2001).

[9] K. Wolke, V. Harms, H. W. Becker, J. W. Hammer, K. L. Kratz, C. Rolfs, U. Schröder, H. P. Trautvetter, M. Wiescher, and A. Wöhr, Z. Phys. A **334**, 491 (1989).

[10] C. E. Rolfs and W. S. Rodney, *Cauldrons in the Cosmos*, 1st ed. (The University of Chicago Press, Chicago, IL, 1988).

[11] K. H. Bray, A. D. Frawley, T. R. Ophel, and F. C. Barker, Nucl. Phys. A **288**, 334 (1977).

[12] R. E. Azuma, E. Uberseder, E. C. Simpson, C. R. Brune, H. Costantini, R. J. de Boer, J. Görres, M. Heil, P. J. LeBlanc, C. Ugalde *et al*., Phys. Rev. C **81**, 045805 (2010).

[13] E. Uberseder, R. deBoer, P. LeBlanc, E. Simpson, and R. Azuma, *AZURE User Manual* (2010), URL azure.nd.edu.

[14] A. Redder, H. W. Becker, H. Lorenz-Wirzba, C. Rolfs, P. Schmalbrock, and H. P. Trautvetter, Z. Phys. A **305**, 325 (1982).

[15] F. Brochard, P. Chevallier, D. Disdier, V. Rauch, and F. Scheibling, J. Phys. (France) **34**, 363 (1973).

[16] J. L. Zyskind and P. D. Parker, Nucl. Phys. A **320**, 404 (1979).

[17] A. Schardt, W. A. Fowler, and C. C. Lauritsen, Phys. Rev. **86**, 527 (1952).

[18] F. B. Hagedorn and J. B. Marion, Phys. Rev. **108**, 1015 (1957).

[19] J. M. Morris, G. W. Kerr, and T. R. Ophel, Nucl. Phys. A **112**, 97 (1968).

[20] D. R. Tilley, H. R. Weller, and C. M. Cheves, Nucl. Phys. A **564**, 1 (1993).

[21] R. J. deBoer, R. E. Azuma, E. Uberseder, J. Görres, G. Imbriani, P. J. LeBlanc, and M. Wiescher, Phys. Rev. C (to be published).